ENVIRONMENTAL RESEARCH
INFRASTRUCTURE AND SUSTAINABILITY

PAPER

Neighborhood-scale air quality, public health, and equity implications of multi-modal vehicle electrification

Maxime A Visa[1,*], Sara F Camilleri[1], Anastasia Montgomery[1], Jordan L Schnell[2,6], Mark Janssen[3], Zachariah E Adelman[3], Susan C Anenberg[4], Emily A Grubert[5] and Daniel E Horton[1,2]

[1] Department of Earth and Planetary Sciences, Northwestern University, Evanston, IL, United States of America
[2] Trienens Institute for Sustainability and Energy, Northwestern University, Evanston, IL, United States of America
[3] Lake Michigan Air Directors Consortium, Rosemont, IL, United States of America
[4] Department of Environmental and Occupational Health, Milken School of Public Health, George Washington University, Washington, DC, United States of America
[5] Keough School of Global Affairs, University of Notre Dame, Notre Dame, IN, United States of America
[6] Now at: Cooperative Institute for Research in Environmental Sciences, University of Colorado, Boulder, NOAA/Global Systems Laboratory, Boulder, CO, United States of America
[*] Author to whom any correspondence should be addressed.

E-mail: maxime.visa@northwestern.edu

Keywords: electric vehicles, transportation, air quality, public health, air pollution, environmental justice

Supplementary material for this article is available online

OPEN ACCESS

RECEIVED
7 April 2023

REVISED
27 July 2023

ACCEPTED FOR PUBLICATION
1 September 2023

PUBLISHED
13 September 2023

Original content from this work may be used under the terms of the Creative Commons Attribution 4.0 licence.

Any further distribution of this work must maintain attribution to the author(s) and the title of the work, journal citation and DOI.

Abstract

Electric vehicles (EVs) constitute just a fraction of the current U.S. transportation fleet; however, EV market share is surging. EV adoption reduces on-road transportation greenhouse gas emissions by decoupling transportation services from petroleum, but impacts on air quality and public health depend on the nature and location of vehicle usage and electricity generation. Here, we use a regulatory-grade chemical transport model and a vehicle-to-electricity generation unit electricity assignment algorithm to characterize neighborhood-scale (∼1 km) air quality and public health benefits and tradeoffs associated with a multi-modal EV transition. We focus on a Chicago-centric regional domain wherein 30% of the on-road transportation fleet is instantaneously electrified and changes in on-road, refueling, and power plant emissions are considered. We find decreases in annual population-weighted domain mean NO_2 (−11.83%) and $PM_{2.5}$ (−2.46%) with concentration reductions of up to −5.1 ppb and −0.98 $\mu g\ m^{-3}$ in urban cores. Conversely, annual population-weighted domain mean maximum daily 8 h average ozone ($MDA8O_3$) concentrations increase +0.64%, with notable intra-urban changes of up to +2.3 ppb. Despite mixed pollutant concentration outcomes, we find overall positive public health outcomes, largely driven by NO_2 concentration reductions that result in outsized mortality rate reductions for people of color, particularly for the Black populations within our domain.

1. Introduction

Air pollutants from the U.S. on-road transportation fleet are a substantial driver of negative public health outcomes [1–3]—a burden that has historically been unjustly and inequitably borne by marginalized population subgroups [4–6]. Annual premature U.S. deaths from on-road fossil fuel-based internal combustion engine (ICE) transportation pollution are estimated to range from ∼12 000 to 31 000 due to ozone and fine particulate matter exposure [7]. Morbidity and mortality impacts from nitrogen dioxide (NO_2) pollution are also substantial [8, 9]. In 2011, ∼37% of U.S. NO_x emissions were attributable to on-road vehicles, with gasoline-powered light-duty vehicles (LDVs) contributing 48% and diesel-powered heavy-duty vehicles (HDVs) 46% [10]. The U.S. transportation sector is likewise responsible for ∼27% of the nation's greenhouse gas (GHG) emissions, making it an essential target for Net Zero mitigation initiatives [11, 12]. Within the U.S. transportation sector, ∼83% of GHG emissions come from on-road sources,

© 2023 The Author(s). Published by IOP Publishing Ltd

including ∼57% from primarily gasoline-powered LDVs, ∼26% from primarily diesel-powered HDVs, and the remaining 17% from off-road sources including aircraft, rail, boat, and other modes [12].

Given the significant contributions of on-road transport to both GHG and pollutant emissions, industry, market, and legislative forces have begun encouraging a transition of the transportation fleet away from fossil-fuel powered ICE vehicles toward non-tailpipe-emitting alternatives such as electric vehicle (EVs) [13]. Because EVs require electricity in lieu of hydrocarbon fuels, EVs have different emission profiles than ICE vehicles. For example, with EV adoption on-road tailpipe emissions are eliminated but emissions associated with additional electricity generation (and in some cases increased brake and tire wear) may increase [14]. However, to date, the air quality and health implications of a multi-modal EV transition have not been widely assessed at the spatial resolutions needed to determine differential exposure between population subgroups (i.e. ∼1 km) [15]—a methodological necessity for environmental justice focused analyses in line with the spirit of the Biden-Harris administration's Justice40 Initiative [16].

While net GHG changes due to an EV transition can be directly related to global concentrations, changes in primary and secondary air pollutants and their health impacts on different population sub-groups are more challenging to assess because of the complicated spatiotemporal relationship between emission sources, the formation, transport, and accumulation of pollutants, and the exposure and susceptibility of different populations. Previous U.S.-focused efforts to understand EV air quality impacts have utilized Earth system simplifying reduced complexity models (RCMs) as well as physics- and chemistry-based chemical transport models (CTMs). RCMs are useful for assessing a range of policy initiatives [17, 18] but unable to predict important health-relevant processes such as secondary pollutant formation (e.g. O_3) and fine temporal scale pollutant extremes (e.g. maximum daily 8 hr average ozone ($MDA8O_3$)). CTMs are capable of simulating the complicated interplay of atmospheric physics and chemistry, but limited by their computational expense. Due to this expense, CTM studies have generally used relatively coarse spatial resolution simulations over the contiguous United States (CONUS) [19–21], with just a few studies employing higher-resolution regionally-focused simulations [22–25], and fewer still that have considered the equity implications of their findings [26].

Prior research has argued that impact- and equity-focused assessments should resolve pollutants at neighborhood-scales (∼1 km) due to an underestimation of impacts when assessed at coarser resolutions [15, 27]. However, production of neighborhood-scale scenario-based CTM simulations and resultant air quality and health impacts have been limited by the lack of both scale-appropriate emissions and population susceptibility data and the substantial computational costs of CTMs. In the particular case of EV assessments, a further challenge has been the lack of an open-source electricity dispatch algorithm that accounts for the battery charging demands of EVs and their attendant electricity generation unit (EGU) emissions. Here, we overcome these barriers by introducing a CONUS-scale vehicle-to-EGU electricity assignment algorithm that we use to inform EGU emissions in regional CTM simulations to constrain the air quality, public health, and equity implications of an instantaneous transition of the transportation fleet from ICE vehicles to EVs. We focus our assessment on a Chicago-centric southern Lake Michigan domain due to the availability of emissions data resolved to 1.3 km [28], the region's prodigious traffic volume [29], and the notable and inequitable air pollution burden historically observed in the region [6, 12, 30].

2. Materials and methods

To determine the air pollutant changes and associated knock-on effects of EV adoption, we compare baseline CTM simulations with sensitivity scenarios that incorporate emission changes consistent with a multi-modal all transport EV transition that includes altered on-road, refueling, and EGU emissions. Baseline and EV adoption simulation scenarios are performed with the two-way coupled Community Multi-Scale Air Quality (CMAQ v5.2) [31] and Weather Research and Forecasting (WRF v3.8) [32] modeling system (WRF-CMAQ) [33]. Baseline simulations are run in nested 12 km, 4 km and 1.3 km domains of decreasing areal extent, with chemical and meteorological boundary conditions for the 1.3 km baseline and EV adoption simulations drawn from the 4 km baseline simulation (i.e. boundary conditions from the 4 km simulation do not incorporate vehicle electrification changes). Comprehensive baseline simulation model configuration and validation details can be found in Montgomery *et al* [34]. The meteorologically-informed 1.3 km baseline emissions are generated using spatial surrogates from the Lake Michigan Air Directors Consortium [35] in the EPA's 2016 Beta platform [36] of the sparse matrix operator kernel emissions (SMOKEs) processing system [37]. Baseline on-road vehicular emission data is sourced at the county-level from the 2016v7.2 National Emissions Inventory [36] but allocated to roadways using LADCO's spatial surrogates and the EPA's MOtor Vehicle Emission Simulator [38]. For both the baseline and EV scenarios, single month simulations from each meteorological quarter are performed (August, October 2018 and January, April 2019) and then averaged to create annualized conditions, in line with previous thematically similar studies [39].

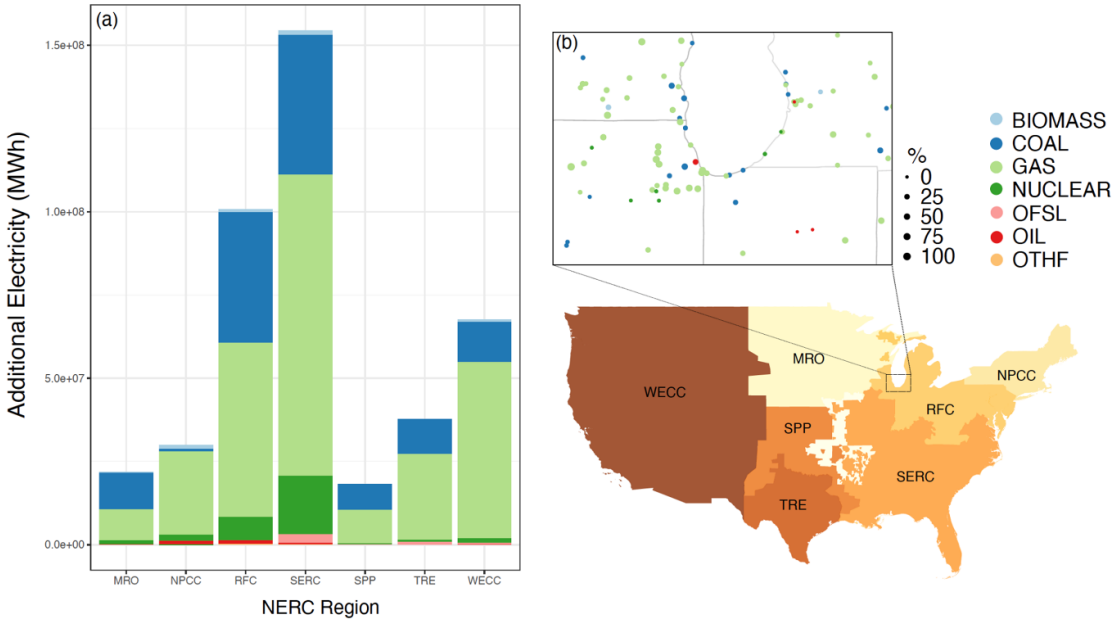

Figure 1. EGU demand. (a) Additional electricity demand by NERC entity and fuel type. (b) Added electricity demand of non-renewable EGUs required to meet an instantaneous transition to 30% multi-modal transportation electrification. EGU sources used to meet the additional demand are determined using a vehicle-to-EGU electricity assignment algorithm (supplemental information). NERC entities are indicated by color shade. The SMOKE emissions modeling framework defines OFSL as 'other fossil fuels' and OTHF as 'other waste-derived fuel sources.'

In our EV adoption scenarios, we modify emissions consistent with the instantaneous electrification of 30% of all on-road transport modes, i.e. motorcycles, all classes of LDVs, and all classes of HDVs (table S2). Vehicles classified as LDVs include primarily gasoline-powered passenger cars and trucks as well as light commercial trucks, while HDVs include primarily diesel-powered intercity, transit, and school buses, refuse trucks, motorhomes, and commercial short- and long-haul trucks. For each mode, 30% of ICE-associated on-road and refueling emissions are removed. Our 30% electrification target for each vehicle mode is not a forecast with a specific time horizon. Projections of EV uptake by mode vary considerably, but have been tending toward a more rapid transition in recent forecasts [40–42]. Critically, our 30% target falls within the decarbonization mid-transition, i.e. a period when consideration of fossil fuel-fired EGUs remains essential [43].

To determine altered EGU emissions due to increased electricity demand from battery charging, we first determine the vehicle miles traveled (VMT) for each vehicle mode in each CONUS county and then reassign 30% of the VMTs to electric VMTs (eVMTs). Given the rapid development of battery technology and the non-specific but future time horizon of our sensitivity scenario, we assume above-current-average battery efficiencies of existing and prominent vehicular technologies for each mode (table S2) and an average gross grid loss of 5.1% [44] to convert eVMTs into a corresponding electricity demand for each county. We then determine EGU sources of added electricity generation (and attendant emissions) using an augmented version of Schnell *et al* [21] vehicle-to-EGU electricity assignment and emissions remapping algorithm. We assume a 2016 grid mix consistent with our emissions inventory and restrict demand to a county's host North American Electric Reliability Organization (NERC) entity. To account for renewable generation, we decrease each NERC entity's added electricity generation demand by the proportion of electricity created by non-renewable sources in that NERC entity. Our augmented vehicle-to-EGU electricity assignment algorithm uses a series of weights to identify which EGUs respond to increased demands. Algorithm weights include: (i) a Boolean NERC screen that restricts fulfillment of demand to EGUs in the same NERC entity as the demanding county (figure 1); (ii) an EGU capacity weight that ensures that EGUs with greater generation capacities preferentially meet demand over EGUs that operate at a high capacity and/or have low generation capabilities; (iii) a distance weight that preferentially selects EGUs closer to the demanding county; and (iv) a ramp rate weight that preferentially selects EGUs with the ability to rapidly meet charging demands. Further details on EGUs that are assigned increased electricity generation (table S3) and our vehicle-to-EGU electricity assignment algorithm can be found in the Supplemental Information.

Once net electricity demand at each CONUS EGU is determined (figure 1), we linearly upscale EGU emissions (table S4). Despite using the vehicle-to-EGU electricity assignment algorithm to constrain CONUS-wide emission changes, we restrict our WRF-CMAQ EV adoption simulations to a Chicago-centric

southern Lake Michigan domain (figure 1(b)) due to the substantial computational expense of neighborhood-scale CTM simulations and the availability of high resolution emission surrogates. For our electrified all transport EV adoption scenario, hereafter, *eAT*, we combine EGU emission changes within our CTM domain together with altered on-road and refueling emissions using the EPA's SMOKE. Lastly, given our use of 2016 grid infrastructure and uncertainties in the pacing of grid decarbonization, we run an additional sensitivity simulation in which EV electricity demands are completely met by emission-free EGUs, hereafter, *eAT_EF*. Air pollutant (i.e. NO_2, $PM_{2.5}$, and O_3) and public health impacts as a function of the modeled EV adoption scenario are determined by subtracting the experimental scenario (*eAT* or *eAT_EF*) from baseline conditions.

We note that our first-order approximation of altered EGU demand and attendant emissions from the U.S. electricity grid does not attempt to explicitly simulate dispatch, nor the myriad drivers and regulations that ultimately determine which EGUs serve load. As such, we make a number of simplifying assumptions. We do not consider time-of-day charging, nor the ramifications associated with daytime versus nighttime charging and its upstream electricity generation. We assume that EGU emissions scale positively and linearly with increased electricity generation. This linear upscaling implicitly assumes that emissions factors for EGUs are constant across operational conditions, which is unlikely to be the case. Although variability in emissions factors is not well reported, EGUs tend to operate at lower efficiency (and thus would be expected to have higher marginal emissions) at low load or while ramping. As such, linear upscaling as used here likely overestimates emissions in contexts where increasing load from EVs drives more hours of operation at full or steady load but underestimates emissions when EVs drive more hours of operation under ramping conditions. Actual conditions will depend substantially on EV load shapes, which in turn are sensitive to policy interventions (e.g. rate design).

While our age weight is used to simulate ramp-rate, we recognize that age is a coarse proxy for responsiveness, and EV charging does not necessarily demand faster ramping per se. In practice, for U.S. fossil EGUs, age is effectively a proxy for plant type and associated ramp rate constraints that highly reduces the dimensionality of analysis (e.g. by not requiring specific disaggregation across multiple types of coal and petroleum fuels; accounting for specific types of pollution controls that are known to affect ramping) and does not require assumptions about ramp rates at the unit level, which are not published. In practice, age fairly closely proxies share of high responsiveness units: natural gas combustion turbines account for 19% of U.S. fossil EGU capacity built prior to 2010, but 36% of US fossil EGU capacity built post 2010 (and 42% built post 2015); natural gas in general accounts for 61% of U.S. fossil EGU capacity built prior to 2010, 84% post-2010, and 99% post-2015 (based on 2018 data) [45]. In addition, the use of age as a coarse proxy embeds other factors that are probably relevant for determining which generators might serve load in the medium term, such as anticipated remaining lifespan, presence of modern pollution controls, efficiency, and proximity to anticipated areas of load growth.

We also make a number of simplifying assumptions with regard to EV use and adoption. We assume that vehicles are charged in the county where they are driven, i.e. we constrain a county's VMTs (and thus electricity demand) to that county and do not consider VMTs driven in a county by a vehicle not residing (and thus charging) in that county; we expect this assumption to mostly hold for LDVs but not for long haul trucks, which could lead to underestimated air quality benefits from increased EGU demand in drive-through counties and overestimated air quality benefits from increased EGU demand at HDV charging hubs. As our scenario instantaneously electrifies 30% of the on-road fleet, we do not model the differential replacement of ICEVs for EVs based on vehicle age, weight, or any other metrics that may expedite or impede the substitution of an ICEV for an EV. We appreciate that instantaneous electrification of the on-road fleet as modeled here does not recognize any emission, pollutant, GHG, and/or health effects of the intermediate electrification states existing between the current EV penetration fraction and a 30% fleet electrification scenario. Further, we recognize that the rates with which different sectors of the U.S. transportation fleet attain 30% electrification will likely differ—i.e. 30% LDV electrification will likely precede 30% HDV electrification—yet we model a homogenous 30% electrification scenario because we believe this assumption to be as limiting as predicting possible differential electrification rates by vehicle class. Additionally, in assigning electricity demands by vehicle class (table S2), we recognize that assigning a single battery efficiency rate (BER) to each representative vehicle type is an assumption that may not represent BER average for each class listed in table S2. Given the rapid development of battery technology and the non-specific but future time horizon of our sensitivity scenario, we assign BERs that are representative of currently available prominent vehicular technologies. For passenger cars and light-duty trucks we chose models that were consistently included in best seller lists that were publicly available in 2021. For modal types with lesser EV market penetration, e.g. refuse trucks and motorhomes, we sourced data from available manufacturer websites. Lastly, we do not perform a life cycle analysis in this study, but rather focus on emissions associated with on-road operations, refueling, and charging. Emissions from EV and EV component (e.g. batteries)

production, resource gathering, transportation, disposal, and other life-cycle-related processes are not considered here, but have been by others [46].

3. Health and environmental justice analyses

To quantify the health impacts following an EV transition, we estimate all-cause mortality associated with long-term NO_2, fine particulate matter ($PM_{2.5}$) and $MDA8O_3$ exposure at the census tract level using annualized mean concentrations computed from hourly simulated data and an epidemiologically derived log-linear concentration-response function (equation (1)):

$$\mathrm{Mort_{CT}} = \mathrm{MR_{CT}} \cdot \ \mathrm{POP_{CT}} \cdot 1 - \exp^{(-\beta \Delta x_{\mathrm{CT}})} \tag{1}$$

where Mort is the all-cause mortality associated with changes in air pollution concentrations following 30% electrification at the census tract level CT, MR is the all-cause mortality rate for ages 30 and over, POP is the population of each census tract, β is the concentration response coefficient relating air pollution levels with increased risk of all-cause mortality and Δx is the annualized change in air pollutant concentration following an EV transition.

Estimated changes in premature NO_2-related all-cause mortality are calculated using a meta-analysis derived relative risk [3] of 1.04 (95% confidence interval (CI): 1.01–1.06) per 10 μg m^{-3} converted to a ppb equivalent using our model-simulated annualized mean temperature of 9.4 °C [34] and an assumed standard pressure of 1013 mb (i.e. 10 μg m^{-3} = 5.04 ppb). Changes in premature $PM_{2.5}$-related all-cause mortality are calculated using a meta-analysis derived relative risk [3] of 1.03 (CI: 1.01–1.04) per 5 μg m^{-3}. For $MDA8O_3$-related all-cause mortality we use the concentration-response function from the updated American Cancer Society Cancer Prevention Study II (ACS CPS-II) with a coefficient of 1.02 (CI: 1.01–1.04) per 10 ppb [47]. Census tract-level population and demographic data were obtained from the American Community Survey (ACS 2015–2019) [48]. Tract-level all-cause mortality rates are derived from USALEEP abridged life tables with modifications for broader use in national health benefit analyses [49]. All health burdens are calculated for ages 30 years and over and uncertainty in health estimates are calculated using the 95% CI associated with each relative risk. The relative risks used here come from two independent studies with distinct scopes. Consequently, relative risks for NO_2 and $PM_{2.5}$ [3] are not adjusted for covariance between pollutants but the relative risk for O_3 is adjusted for $PM_{2.5}$ with associations between O_3 and all-cause mortality persisting following NO_2 adjustment. Given these differences between the sources of the relative risks used in this study, we do not estimate the additive health impacts from all three pollutants to avoid overestimation of the total burden.

4. Results and discussion

4.1. Electricity assignment and emission changes

Due to the interconnected nature of the U.S. electric grid, we use our vehicle-to-EGU electricity assignment algorithm to first compute the additional electricity demand required to meet EV battery charging needs assuming 30% multi-modal vehicle electrification across all of CONUS. We then determine the EGU sources used to meet that additional demand (figure 1). We estimate that the annual battery charging demands for 30% all transport electrification for CONUS are 5.01 $\times$ 10^8 MWh, an increase of 21.3% from baseline demand. Using annual EGU operative capacity averages as well as temporally-averaged increased EGU demands—i.e. not considering time of day charging nor peak demand—we find that this magnitude of demand could be met with 2016 EGU infrastructure capacity. Amongst non-renewable CONUS EGUs to which the algorithm assigns electricity, 61.8% of demand is met by natural gas-fired plants, 28.6% by coal-fired plants, 6.8% by nuclear plants, 1.1% by biomass-fired plants, 0.6% by oil-fired plants, and the remaining ~1% by plants using other fuel types, to include OFSL (other fossil fuels) and OTHF (other waste-derived fuel sources) [44] (figure 1).

Given the regional focus of our CTM experiments, we also characterize changes at EGUs that reside within our Chicago-centric, southern Lake Michigan CTM domain boundaries (figure 1(b)), which are responsible for supplying 74.5% of the electricity the *eAT* fleet in our domain demands. In our CTM domain, we find that coal-fired EGUs are assigned 8.0 TWh (38.7%), gas-fired EGUs 12.7 TWh (61.1%), oil-fired EGUs 816 MWh (0.000%), biomass-fired EGUs 14.7 GWh (0.001%), and other fuel type EGUs 13.3 GWh (0.001%). Within the CTM domain, we estimate an average annual EGU demand increase of 32.7% (figure 1(b)) with domain EGU CO_2 emissions increasing ~14.1 M tonnes yr^{-1}. However, EGU CO_2 emissions increases are accompanied by annual on-road and refueling emission reductions of ~29.2 M tonnes yr^{-1}, which on net reduces CO_2 emissions over our CTM domain by ~15.1 M tonnes yr^{-1}.

Compared to the baseline scenario, we find that net emissions of most other pollutants also decrease over our domain, with the exception of SO_2, which increases (+6.06%; table S4), primarily due to increased generation at coal-fired EGUs (figure S1). The most prominent pollutant decreases in the 30% *eAT* scenario are of carbon monoxide (−17.17%) and NO_2 (−15.06%), with NO_x (−13.76%), NO (−13.53%), volatile organic compounds (−8.27%), and primary elemental carbon decreases also notable (−8.52%; table S4). In the *eAT_EF* scenario, added EGU-attributable CO_2 emissions are reduced to 0 tonnes yr^{-1}, which increases net CO_2 reductions to the full on-road reduction of 29.2 M tonnes yr^{-1}.

4.2. Air pollutant changes resulting from 30% multi-modal EV transition

To constrain criteria pollutant changes resulting from an instantaneous 30% all transport EV transition, we compare baseline CTM simulations to simulations that incorporate the altered on-road, refueling infrastructure, and EGU emissions discussed above. For the 30% *eAT* scenario we find domain average decreases in all criteria pollutants: that is, NO_2 decreases −0.29 ppb (−10.3%), $MDA8O_3$ decreases −0.05 ppb (−0.1%), and $PM_{2.5}$ decreases −0.09 $\mu g\ m^{-3}$ (−1.6%; figure 2). Both NO_2 (figures 2(b)) and $PM_{2.5}$ (figure 2(f)) decrease over the full domain, whereas $MDA8O_3$ increases in high-trafficked and high-population locales (figure 2(d)). Within grid cells that contain EGUs, mean decreases in NO_2 and $PM_{2.5}$ are simulated, despite increased electricity generation. For the *eAT_EF* scenario, we also find domain average decreases in NO_2 (−0.31 ppb; −11.0%), $MDA8O_3$ (−0.05 ppb; −0.1%), and $PM_{2.5}$ (−0.11 $\mu g\ m^{-3}$; −2.0%) though the added pollutant concentration benefits of emission-free EGUs are marginal (−0.01 ppb, −0.001 ppb, and −0.01 $\mu g\ m^{-3}$, respectively; figure S2). Given the incremental changes simulated in the *eAT_EF* scenario, we primarily focus our results on the *eAT* scenario.

In the *eAT* scenario, annual average changes in NO_2 concentrations are well defined over interstates and roadways (figure 2(b)), with the greatest reductions coincident with NO_x emission sources, consistent with the short lifetime of NO_2 in the atmosphere. In the most populous county of our domain, Cook County—home of Chicago—average annual baseline NO_2 concentrations reach 28 ppb, but concentrations in the *eAT* scenario decrease up to −5.1 ppb, with an average decrease of 10.3% for the full domain (figures 2(a) and (b)). We find that the mean decrease in NO_2 over the domain is −0.29 ppb, while population-weighted NO_2 decreases −0.95 ppb (table S5), demonstrating that greater NO_2 decreases coincide with higher population density.

Across our modeling domain, we observe mixed results with regard to changes in surface-level $MDA8O_3$ concentrations for the *eAT* scenario (figures 2(d) and S3). While high-density areas show increases in $MDA8O_3$ concentrations, $MDA8O_3$ decreases of up to −0.6 ppb (figure 2(d)) are simulated in less populated, rural areas. Domain average ambient $MDA8O_3$ concentrations decrease −0.05 ppb, while population-weighted $MDA8O_3$ increases 0.29 ppb (table S5). We observe the greatest $MDA8O_3$ increases (figure 2(d)) where baseline $MDA8O_3$ levels are lowest (figure 2(c)), the opposite pattern of our simulated NO_2 changes. Using WHO guidelines of 50 ppb [50], we find that the *eAT* scenario adds up to nine days above recommended ozone levels in some Cook County grid cells (figure 3(a)). Other counties in the domain demonstrate mixed $MDA8O_3$ results, with some grid cells showing decreases in days above suggested ozone guidelines (figure 3). To demonstrate, we highlight one county from each of the states in our domain. In Milwaukee County, WI we find notable increases in days above WHO recommended $MDA8O_3$ levels in some grid cells (figure 3(b)), but in Kent County, MI—home of Grand Rapids (figure 3(c))—and in Noble County, IN (figure 3(d)) we largely find fewer grid cells with days above recommended levels. Increases in $MDA8O_3$ over roadways and urban cores are driven by the reduction in NO_x emissions, which leads to reduced O_3 titration by NO, consistent with the VOC-limited regime we simulate in these areas in the baseline for most of the year [34]. We note that in NO_x-limited rural regions of our domain, simulated summer (August) and spring (April) month $MDA8O_3$ changes differ from those simulated in fall and winter months (October & January; figure S3).

In the *eAT* scenario, we find a domain-wide reduction in $PM_{2.5}$ concentrations with notable decreases along highways and within the Chicago metropolitan area (figure 2(f)). Simulated $PM_{2.5}$ decreases are more diffuse and widespread than NO_2 decreases, consistent with the longer average lifetime of many PM species [51]. Similar to NO_2, we find a domain average decrease in $PM_{2.5}$ of −0.09 $\mu g\ m^{-3}$ but a population-weighted $PM_{2.5}$ decrease of −0.19 $\mu g\ m^{-3}$ (table S5), demonstrating the strong link between population density and pollutant concentrations. Some previous EV transition studies have found regionally isolated increases in $PM_{2.5}$ concentrations due to increased EGU demand and attendant emissions [21]. In our *eAT* scenario we do not simulate $PM_{2.5}$ increases, but do find increases in some $PM_{2.5}$ precursor species. That is, we find a domain average increase in SO_2 concentrations—a precursor of sulfate aerosols—of 3.8 ppt (figure S1). However, we find that EGU $PM_{2.5}$ constituent increases are offset by decreases in other $PM_{2.5}$ species, such that on-road benefits outweigh point source disbenefits vis a vis overall $PM_{2.5}$ pollution (figure S1, table S4).

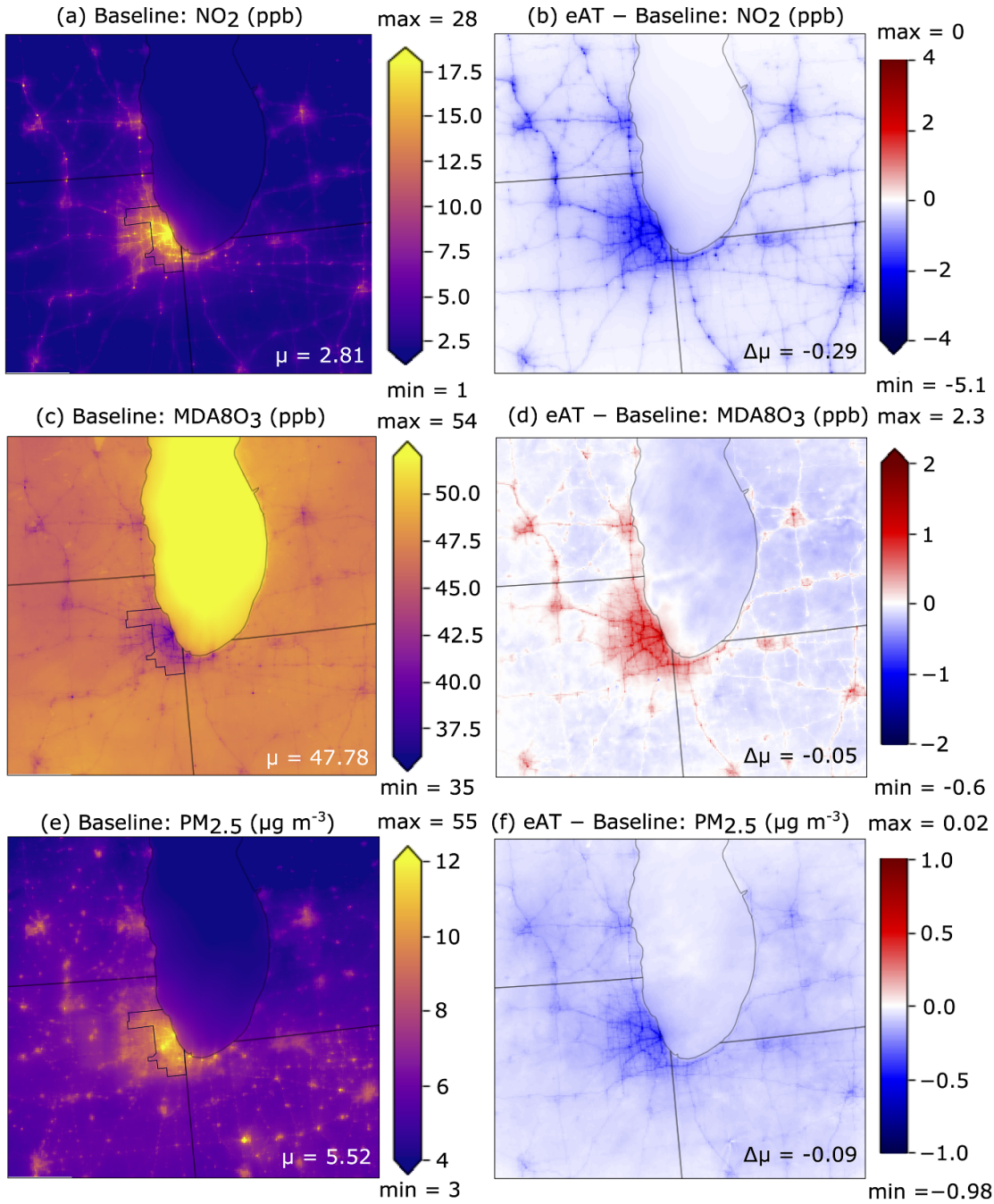

Figure 2. Changes in pollutant concentrations: Annualized mean WRF-CMAQ simulated baseline pollutant concentrations (a), (c), (e) and differences that result from 30% multi-modal all transport EV adoption (b), (d), (f). We indicate the geographic boundary of Cook County, IL—home to Chicago—on the left hand panels. Domain-average (μ) concentrations and concentration changes ($\Delta\mu$) are included in each panel. All WRF-CMAQ simulations are performed using a 1.3 km spatial resolution.

4.3. Public health implications of pollutant changes

We assess changes in health outcomes resulting from the *eAT* scenario at the census tract level, which is made possible by our CTM simulation's spatial resolution and USALEEP census tract level all-cause mortality rates [49]. Although we find both benefits and detriments to public health in the *eAT* scenario within our modeling domain, outcomes are primarily positive (figure 4). We estimate that domain-wide NO_2 reductions decrease premature deaths/yr by 1120 (CI: 280, 1680), while $PM_{2.5}$ reductions lead to 170 (CI:60, 290) avoided deaths/yr. Domain-wide NO_2 and $PM_{2.5}$ changes benefit public health, however, simulated surface-level $MDA8O_3$ increases have negative consequences, contributing to an estimated 80 (CI: 40, 170) additional premature deaths/yr. Given the modest pollutant concentration differences in the *eAT_EF* scenario compared to the *eAT* scenario, additional health benefits are marginal: benefits from reduced NO_2 increase to 1150 (CI: 290, 1730) avoided premature deaths/yr, benefits from reduced $PM_{2.5}$ increase to 190

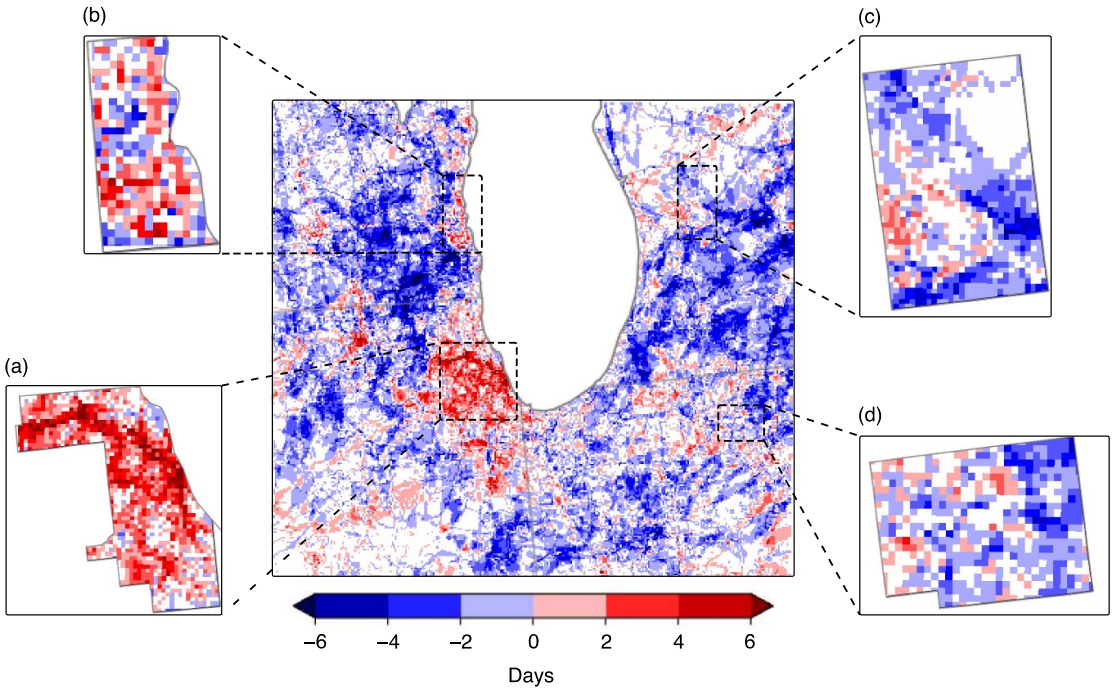

Figure 3. Added ozone days above 50 ppb Additional days above World Health Organization (WHO) recommended $MDA8O_3$ concentrations in the *eAT* scenario relative to the baseline simulation. WHO ozone guidelines suggest a 50 ppb threshold. We highlight the following counties: (a) Cook, IL, (b) Milwaukee, WI, (c) Kent, MI, and (d) Noble, IN.

(CI: 60, 320) avoided premature deaths/yr, and disbenefits from increased $MDA8O_3$ increase to 90 (CI: 40, 180) additional premature deaths/yr (table S6). In addition, given the influence of meteorological natural variability on air quality and the limited temporal extent of our CTM simulations, in figure S4 we compute health impact metrics for each constituent modeling month included in the annualized average estimates presented above. This month-by-month analysis reveals largely consistent changes in sign across seasons and only moderate changes in magnitude. The notable exception is found in summer, where EV adoption results in reduced $MDA8O_3$ concentrations and fewer premature deaths.

While pollutant concentration differences within census tracts are important in determining changes in attributable mortality, underlying all-cause mortality rates also play an important role in determining health outcomes. We note that census tracts with large changes in attributable mortality due to EV adoption do not necessarily correspond to census tracts with large simulated changes in pollutant concentrations (figures 2(b) and 4(a)). To explain this discrepancy and highlight the ability of our high resolution CTM simulations to resolve intra-urban heterogeneities we focus on census tract level NO_2 outcomes over Cook County, IL, where NO_2 is found to decrease over all tracts, albeit non-uniformly (figure 5(b)). We find reductions in NO_2-related all-cause mortality rate due to EV adoption in all Cook County census tracts (figure 5(a)). However, magnitudes are elevated in tracts that have either (i) larger NO_2 reductions and higher mortality rates (dark green; figure 5(d)) or (ii) higher mortality rates and smaller NO_2 reductions (dark yellow; figure 5(d)). In contrast, magnitudes are lower in tracts that have either (iii) smaller NO_2 reductions and lower mortality rates (light gray; figure 5(d)) or (iv) lower mortality rates but larger NO_2 reductions (dark blue; figure 5(d)). Examples of each follow: (i) on the west side of Cook County, highways and industrial areas are prevalent and census tracts have both large NO_2 reductions and high mortality rates which results in overall large health benefits with EV adoption (figure 5(d)); (ii) on the southwest side of Cook County, larger health benefits of EV adoption are driven by large underlying mortality rates despite smaller NO_2 reductions (figure 5(d)); (iii) in the north and northwestern suburbs, low mortality rates and smaller NO_2 reductions result in only limited estimated NO_2 mortality reduction; and (iv) in Chicago's inner core, i.e. 'the Loop' low mortality rates lead to lesser estimated NO_2 mortality rate reductions despite substantial simulated NO_2 concentration decreases.

These nuanced NO_2-focused results highlight the beneficial synergy of working with both high resolution health data (i.e. mortality rates) and neighborhood scale air quality simulations, as each is essential to elucidate intra-urban heterogeneities in estimated air pollution-related health impacts. In addition, our finding that some of the largest health benefits occur distal to the largest pollution decreases is notable for the challenges it presents in designing effective pollutant-focused amelioration policies as well as its parallels

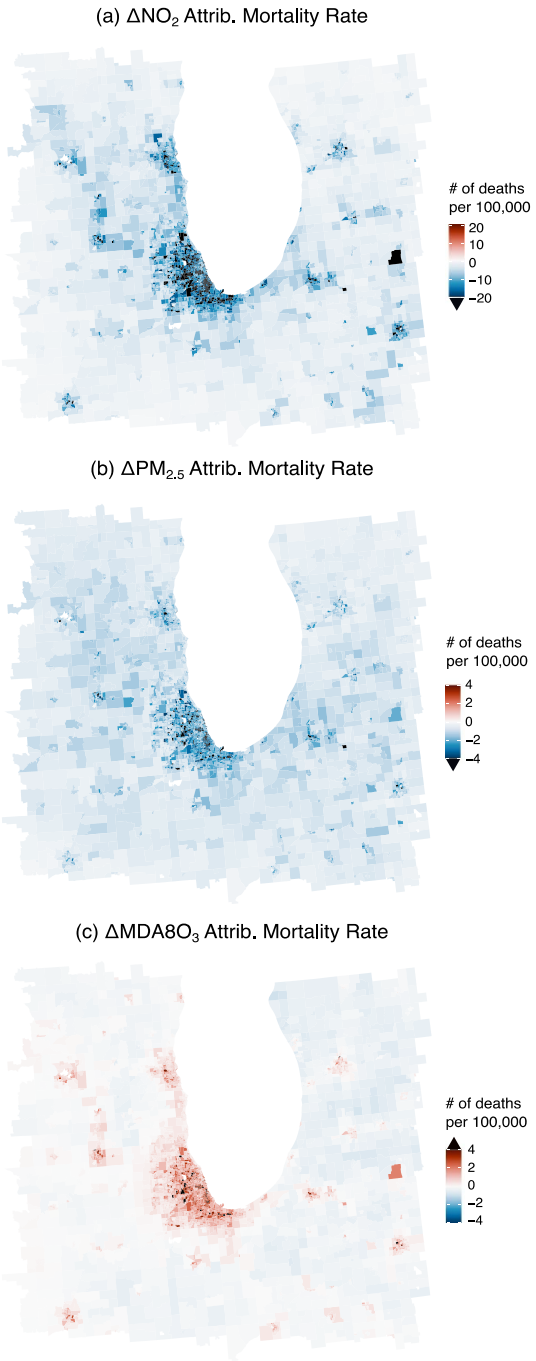

Figure 4. Census tract-level changes in premature all-cause mortality rate (per 100 000 people) among adults 30 years and older in the *eAT* scenario census tract level premature per year death rate increases or decreases relative to the baseline scenario associated with concentration changes in annual average (a) NO_2, (b) $PM_{2.5}$, and (c) $MDA8O_3$.

with recent findings that social-demographic factors may play the predominant role in shaping the future global health burden of air pollution [52].

4.4. Equity implications

Given the historically disproportionate poor air quality burden borne by disadvantaged U.S. communities, in concert with recent policy initiatives championing environmental justice [16], we assess the distribution of benefits and disbenefits of our EV adoption scenarios across population subgroups within Cook County. To perform this equity-focused analysis we analyze the racial and ethnic composition for each pollutant concentration difference decile and repeat this analysis for changes in each pollutant-attributable mortality rate decile (figure 6). For Cook County, we find that people of color comprise the majority (>∼54%; figure 6(a)) of the racial/ethnic composition for all NO_2 difference deciles, representative of the racial/ethnic make-up of Cook County, with predominantly Hispanic/Latino populations in the northwest and southwest

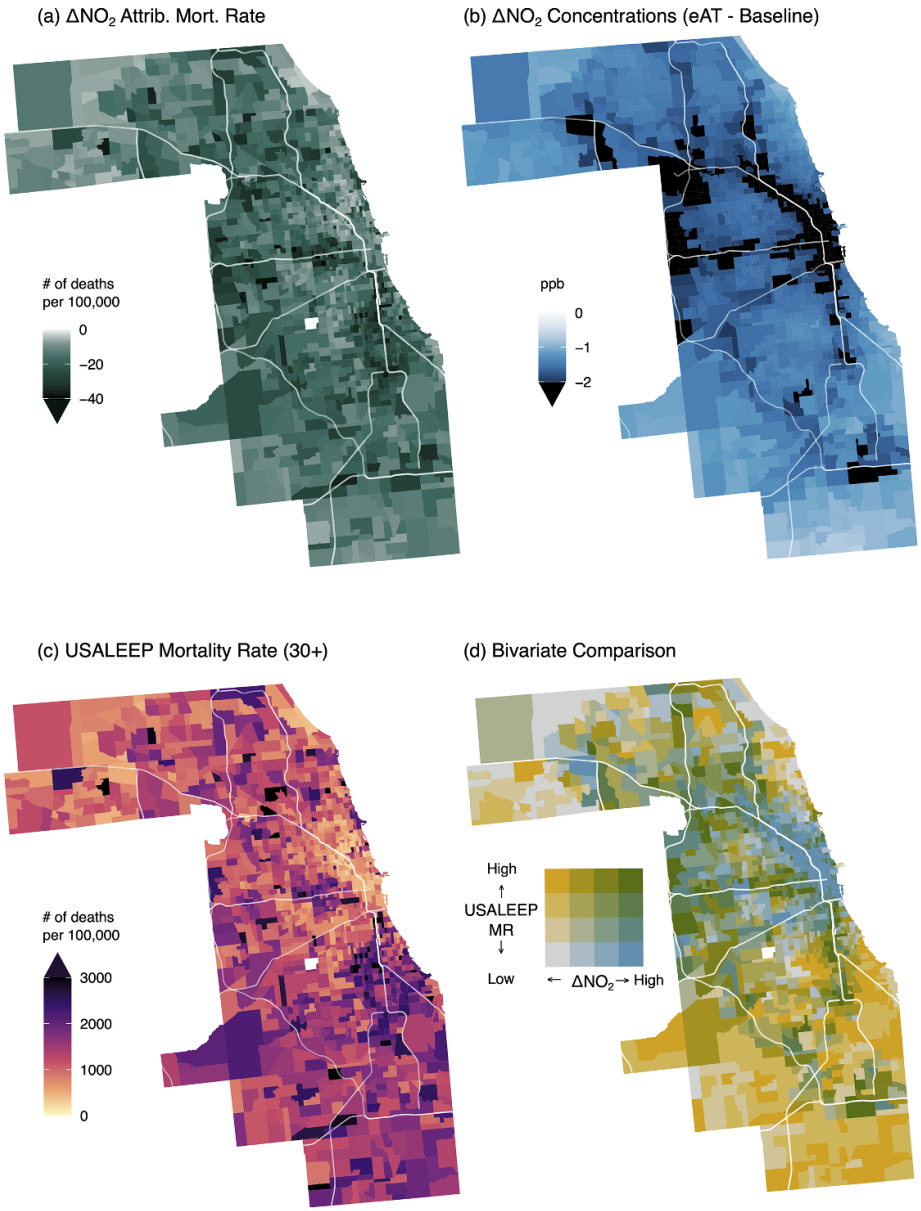

Figure 5. Bivariate analysis of NO_2 Differences and Mortality Rates Census tract level analyses of Cook County, IL depicting the relationships between (a) estimated NO_2 attributable mortality rate differences, (b) simulated NO_2 concentration changes from baseline to *eAT* scenario, (c) 30 year old and over mortality rate (MR), and (d) bivariate overlap between MR and NO_2 changes.

and Black populations in the west and south. Similarly, people of color benefit the most from $PM_{2.5}$ reductions across most deciles (>52%, 1st to 9th decile; figure 6(a)) however, unlike NO_2, ∼51% of the Cook County population exposed to the highest $PM_{2.5}$ reductions is non-Hispanic White (10th decile, figure 6(b)). Given the simulated increases in $MDA8O_3$ concentrations due to complex non-linear chemistry, we find that the Black and Hispanic/Latino populations are overrepresented in areas with $MDA8O_3$ increases across most deciles (>57%; figure 6(c)).

The disparities in health benefits associated with decreases in NO_2 and $PM_{2.5}$ concentrations (figures 6 (d) and (e)) are more distinct as compared to disparities in air pollution exposure differences (figures 6(a) and (b)). For both NO_2 and $PM_{2.5}$, we note small health benefits in predominantly non-Hispanic White populations (∼56% 1st decile figures 6(d) and (e)) but large health benefits for people of color particularly, the Black population (>55% 10th decile figures 6(d) and (e)). Differences in the racial/ethnic composition between air pollution (figures 6(a) and (b)) and health burden deciles (figures 6(d) and (e)) reflect the influence of population susceptibility incorporated in health burden estimates (refer to figure 5 discussion). Higher baseline mortality rates in minoritized subgroups such as the Black population (e.g. figure 5(c)), in conjunction with moderate to large reductions in air pollution exposure within these census tracts (figures 6(a) and (b)) both contribute to this outsized impact (figures 6(d) and (e)). We also note higher

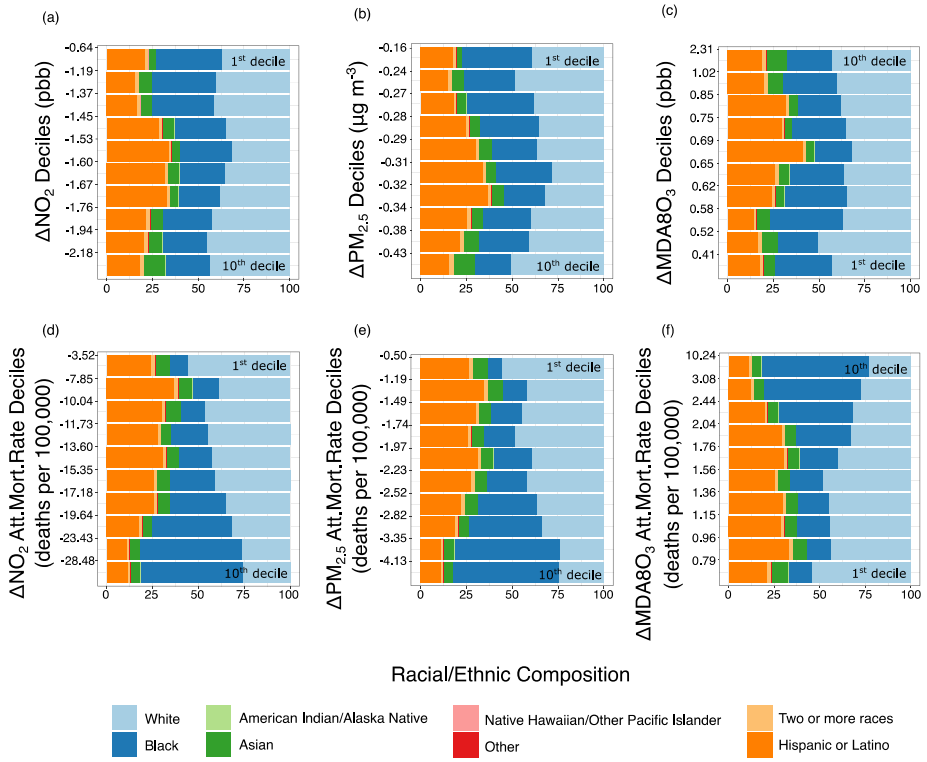

Figure 6. Pollutant and health impacts by demographic change in pollutant concentration (a)–(c) and change in attributable mortality rate per 100 000 (d)–(f) by racial/ethnic composition over Cook County, IL.

estimated NO_2-related health benefits as compared to $PM_{2.5}$ which is largely driven by larger reductions in NO_2 concentrations and different relative risks (refer to figure 2). Health damages associated with increases in $MDA8O_3$ concentrations are smallest for the White population (∼54%; 1st decile figure 6(f)) but largest for the Black population (∼59%; 10th decile) however, the magnitude of the largest $MDA8O_3$-related health damages (10th decile figure 6(f)) is ∼2.8 times smaller compared to the largest NO_2-related health benefits within these same minoritized communities.

4.5. Economic implications

To add additional context to the simulated pollutant concentration changes and resultant health outcomes due to 30% all transport electrification, we also assess the economic implications of our EV transition scenarios. We perform our economic analysis over the full CTM domain. To quantify economic implications we assess the monetary value of both health outcomes and CO_2 emission changes, commonly referred to as co-benefits [53]. We use a \$9.6 M (USD2017) valuation of statistical life [54, 55] to assess the economic impact of domain-wide health outcomes. In the *eAT* scenario, we find savings of \$10.75 B yr^{-1} due to fewer NO_2-related deaths and \$1.63 B yr^{-1} due to fewer $PM_{2.5}$-related deaths, but added expenditures of \$768 M yr^{-1} due to increases in surface-level $MDA8O_3$-driven deaths. The *eAT_EF* scenario offers greater health benefits than the *eAT* scenario, thus we find additional savings of \$288 M yr^{-1} corresponding to fewer NO_2-related deaths, \$192 M yr^{-1} corresponding to fewer $PM_{2.5}$-related deaths, and \$96 M yr^{-1} incurred due to $MDA8O_3$-related deaths. For CO_2 emission changes, we apply Rennert *et al* [56] estimate of the social cost of carbon (\$185/tCO_2) which aims to quantify the socioeconomic impact of GHG emissions. For our 30% *eAT* scenario we find a domain-wide benefit of \$2.8 B yr^{-1} from the 15.1 M tonnes yr^{-1} reduction in CO_2 emissions. In the *eAT_EF* scenario, the SCC benefit increases to \$5.4 B yr^{-1}, due to CO_2 emission reductions of 29.2 M tonnes yr^{-1}. Due to the uncertain nature of the SCC, we note that economic benefits vary greatly depending on an SCC's underlying assumptions [57]. For example, the current SCC endorsed by the U.S. EPA, \$51/tCO_2, sits well below Rennert *et al's* SCC of \$185/tCO_2 [58]. To avoid overestimation of the overall economic impact associated with the health benefits and disbenefits of *eAT* and *eAT_EF* we do not aggregate the economic impacts from all three pollutants as mortality risks are not independent of each other, especially for correlated pollutants such as NO_2 and $PM_{2.5}$. However, we note that estimated savings from reduced negative NO_2-related health outcomes are larger compared to savings from CO_2 reductions even when using a considerably high SCC, a result consistent with previous studies showing outsized monetized health co-benefits compared to GHG abatement costs [59].

5. Discussion

Our 30% multi-modal EV transition simulation results demonstrate that a one-to-one transition of ICE VMTs to eVMTs has largely positive GHG, air pollutant, public health, and equity benefits. Overall positive health benefits are primarily driven by reductions in NO_2 that result in a decrease in over 1100 deaths yr^{-1} over our CTM domain, substantially more than $PM_{2.5}$ -related health benefits or $MDA8O_3$-related disbenefits. NO_2 reduction across all deciles mostly benefit people of color with large health benefits for Black populations. Our finding of substantial EV adoption-NO_2 benefits is notable given (i) emerging epidemiological research indicating that NO_2 impacts may be independent of impacts from co-pollutants like $PM_{2.5}$ [9, 60, 61], (ii) strong evidence of other unfavorable NO_2-related health impacts [2, 8, 62], and (iii) the potential for the U.S. EPA's transportation-focused Regulatory Impact Analyses to assess holistic measures of air quality, as opposed to individual pollutant exceedances. Despite overall positive benefits, our finding of increases in O_3 pollution in high-population areas—while not surprising [20, 23, 25]—is an EV adoption tradeoff that bears consideration, particularly in regions where marginal concentration increases could lead to regulatory threshold exceedances (figure 3), or in locations where pollutant-specific environmental justice concerns are paramount.

Computed estimates of pollutant exposure and health impacts reported herein are model-based (i.e. WRF-CMAQ) and subject to model biases and model errors. While we validated our baseline simulations against available observations (table S1; Montgomery *et al* [34]), it should be noted that (a) our model grid cell to *in situ* observation comparisons occur at no more than 0.14% of our domain's grid cells ($n = 90\,720$) due to relatively few EPA AQS stations, (b) our baseline simulations generally meet suggested community benchmarks [63], and (c) most of the analyses presented herein rely on sensitivity experiment differences, i.e. changes that add to or subtract from baseline conditions and would therefore be hypothetically similar if the baseline simulations had higher fidelity to station observations. A noted exception to this caveat is our $MDA8O_3$ exceedances analyses, wherein concentrations beyond a threshold are computed. It should be noted, however, that Montgomery *et al* [34] report greater biases at lower O_3 concentrations than high.

Our use of a chemical transport and emissions model with region-specific sub-grid scale emission surrogates has facilitated our fine-scale characterization of pollutant changes due to EV adoption. To assess health impacts, we assume that populations within each census tract are only exposed to the air pollution concentrations within that census tract and do not consider population mobility. Epidemiological studies focusing on long-term exposures generally assign air pollution exposure to residential, school and/or work addresses as representation of spatial contrasts in air pollution over longer time periods is more important than day to day variability, typical of short-term exposure studies. We note that the spatial resolution used here of 1.3 km is coarser than finer scale studies characterizing near-roadway pollution (<1 km) [64–66]. However, we note that increasing model spatial resolution to finer scales beyond 1 km can come at the expense of exposure misclassification as the assumption of population mobility becomes more important. Additionally, the resolution of our estimated health impacts is limited by the resolution of available health data, that is at the census tract level. In our health impact assessment we use 1.3 km air pollution concentrations to estimate health burdens in line with the spatial resolution selection criteria used by the HEI to generate the RRs used here (typically <5 km) [3].

Our EV adoption scenarios consider a critical moment in the dynamic decarbonization of the U.S. electric grid, i.e. a mid-transition moment wherein consideration of fossil fuel-fired EGUs remains critical [43]. Given uncertainties in the pace of grid decarbonization, our experimental design brackets overly conservative and overly ambitious grid evolution scenarios, i.e. our *eAT* scenario assumes added electricity demand is met by 2016 infrastructure while our *eAT_EF* scenario assumes emission-free generation. Results from our EV adoption scenarios indicate that from the perspective of GHG emissions, swapping fossil fuel-fired EGUs for emission-free electricity generation has a profound impact, i.e. CO_2 emission reductions and their economic valuation double. However, from the perspective of air pollutants, over our Chicago-centric domain only marginal air quality and public health gains are realized when fossil fuel-fired EGUs are swapped for emission-free electricity generation sources (tables S5 and S6). Additionally, we note that decreases in NO_2 and $PM_{2.5}$ concentrations that predominantly occur in urban counties, do not occur at the expense of increased air pollutant concentrations near EGU locations within our CTM domain; even in grid cells containing EGUs, NO_2 and $PM_{2.5}$ concentrations decrease—despite higher EGU emissions (table S4)—due to contemporaneous decreases in on-road pollution in these same grid cells. However, it should be noted that while 74.5% (27.8 TWh) of the electricity demand required to meet 30% vehicle electrification is sourced from EGUs within our CTM domain, the remaining 25.5% (7.1 TWh) is sourced from EGUs outside the CTM domain, where we are unable to simulate primary and secondary pollutant concentrations or assess health impacts. Lastly, here we present air quality changes brought about by altered on-road tailpipe and refueling emissions; however, we do not consider any increased contributions to on-road non-exhaust

emissions such as brake wear, tire wear, road wear and road dust resuspension which contribute to on-road PM and which might increase in the future as heavy batteries in EVs weigh more compared to ICEs, particularly for vehicles with a larger driving range [14].

6. Conclusion

While our results demonstrate that shifting the transportation fleet to EVs leads to largely positive outcomes—some of which directly address longstanding environmental injustices—it is important to note that other methods of transportation reform and urban design are likely to offer greater benefits than an EV transition alone. Methods that prioritize physical and mental health, energy efficiency, and environmental benefits, i.e. methods that increase active transport and mass transit while decreasing vehicle dependency, are needed. Indeed a one-to-one replacement of ICE VMTs with eVMTs will not be sufficient to meet international decarbonization goals, and a structural re-thinking, re-design, and re-engineering of transportation systems will be required [67, 68].

Data availability statement

The data that support the findings of this study are openly available at the following URL/DOI: https://github.com/NU-CCRG.

Acknowledgments

Research reported here was supported by the U.S. National Science Foundation Grants CBET-1848683 and CAREER:CAS-Climate-2239834 to DEH, an Environmental Defense Fund (EDF) grant to DEH, a McCormick Center for Engineering Sustainability and Resilience seed grant to DEH, the Ubben Program for Carbon and Climate Science postdoctoral fellowship to J L S, The Data Science fellowship from the National Science Foundation Research Traineeship and Northwestern Integrated Data-Driven Discovery in Earth and Astrophysical Sciences to A M, and undergraduate research grants from Northwestern University's Office of Undergraduate Research and Weinberg College of Arts and Sciences' Baker Program in Undergraduate Research to M A V. This research was supported in part through the computational resources and staff contributions provided for the Quest high performance computing facility at Northwestern University which is jointly supported by the Office of the Provost, the Office for Research, and Northwestern University Information Technology. We thank William Raich, Henry Roman, and Melanie Jackson from the Industrial Economic as well as Neal Fann, Elizabeth Chan and Ali Kamal from the U.S. EPA for deriving and providing the census tract-level all-cause mortality rates used in this study.

Funding

Environmental Defense Fund; U.S. National Science Foundation Grants CBET-1848683 and CAREER:CAS-Climate-2239834

ORCID iDs

Maxime A Visa https://orcid.org/0000-0001-6437-8043
Sara F Camilleri https://orcid.org/0000-0002-4299-8644
Anastasia Montgomery https://orcid.org/0000-0001-7742-9102
Jordan L Schnell https://orcid.org/0000-0002-4072-4033
Susan C Anenberg https://orcid.org/0000-0002-9668-603X
Emily A Grubert https://orcid.org/0000-0003-2196-7571
Daniel E Horton https://orcid.org/0000-0002-2065-4517

References

[1] Anenberg S, Miller J, Henze D and Minjares R 2019 A global snapshot of the air pollution-related health impacts of transportation sector emissions in 2010 and 2015 (ICCT) (available at: https://trid.trb.org/view/1591968)
[2] Anenberg S C, Mohegh A, Goldberg D L, Kerr G H, Brauer M, Burkart K, Hystad P, Larkin A, Wozniak S and Lamsal L 2022 Long-term trends in urban NO_2 concentrations and associated paediatric asthma incidence: estimates from global datasets *Lancet Planet. Health* **6** e49–58
[3] HEI 2022 Systematic review and meta-analysis of selected health effects of long-term exposure to traffic-related air pollution (Special Report 23; Health Effects Institute) (available at: www.healtheffects.org/publication/systematic-review-and-meta-analysis-selected-health-effects-long-term-exposure-traffic)

[4] Castillo M D, Kinney P L, Southerland V, Arno C A, Crawford K, van Donkelaar A, Hammer M, Martin R V and Anenberg S C 2021 Estimating intra-urban inequities in $PM_{2.5}$-Attributable health impacts: a case study for Washington, DC *GeoHealth* **5** e2021GH000431
[5] Colmer J, Hardman I, Shimshack J and Voorheis J 2020 Disparities in $PM_{2.5}$ air pollution in the United States *Science* **369** 575–8
[6] Kerr G H, Goldberg D L and Anenberg S C 2021 COVID-19 pandemic reveals persistent disparities in nitrogen dioxide pollution *Proc. Natl Acad. Sci.* **118** e2022409118
[7] Davidson K, Fann N, Zawacki M, Fulcher C and Baker K R 2020 The recent and future health burden of the U.S. Mobile sector apportioned by source *Environ. Res. Lett.* **15** 075009
[8] Anenberg S C *et al* 2018 Estimates of the global burden of ambient $PM_{2.5}$, Ozone, and NO_2 on Asthma Incidence and emergency room visits *Environ. Health Perspect.* **126** 107004
[9] Song J, Wang Y, Zhang Q, Qin W, Pan R, Yi W, Xu Z, Cheng J and Su H 2023 Premature mortality attributable to NO_2 exposure in cities and the role of built environment: a global analysis *Sci. Total Environ.* **866** 161395
[10] U.S. EPA Integrated science assessment (ISA) for oxides of nitrogen—health criteria (Final Report, Jan 2016) (U.S. EPA) (available at: https://cfpub.epa.gov/ncea/isa/recordisplay.cfm deid=310879)
[11] United Nations Net zero coalition (United Nations) (available at: www.un.org/en/climatechange/net-zero-coalition)
[12] U.S. EPA 2022 Inventory of U.S. greenhouse gas emissions and sinks: 1990–2020 EPA 430-R-22-003 (U.S. Environmental Protection Agency)
[13] Karnowski S California plans to ban new gas cars by 2035. Will 17 states follow? (USA Today) (available at: www.usatoday.com/story/news/nation/2022/09/03/california-gas-car-ban-17-states-follow/7987248001/)
[14] Carey J 2023 The other benefit of electric vehicles *Proc. Natl Acad. Sci.* **120** e2220923120
[15] Clark L P, Harris M H, Apte J S and Marshall J D 2022 National and intraurban air pollution exposure disparity estimates in the United States: impact of data-aggregation spatial scale *Environ. Sci. Technol. Lett.* **9** 786–91
[16] The White House Justice40 Initiative | Environmental Justice (The White House) (available at: www.whitehouse.gov/environmentaljustice/justice40/)
[17] Tessum C W, Hill J D and Marshall J D 2017 InMAP: a model for air pollution interventions *PLoS One* **12** e0176131
[18] Holland S P, Mansur E T, Muller N Z and Yates A J 2016 Are there environmental benefits from driving electric vehicles? The importance of local factors *Am. Econ. Rev.* **106** 3700–29
[19] Nopmongcol U, Grant J, Knipping E, Alexander M, Schurhoff R, Young D, Jung J, Shah T and Yarwood G 2017 Air quality impacts of electrifying vehicles and equipment across the United States *Environ. Sci. Technol.* **51** 2830–7
[20] Peters D R, Schnell J L, Kinney P L, Naik V and Horton D E 2020 Public health and climate benefits and trade-offs of U.S. vehicle electrification *GeoHealth* **4** e2020GH000275
[21] Schnell J L, Naik V, Horowitz L W, Paulot F, Ginoux P, Zhao M and Horton D E 2019 Air quality impacts from the electrification of light-duty passenger vehicles in the United States *Atmos. Environ.* **208** 95–102
[22] Brinkman G L, Denholm P, Hannigan M P and Milford J B 2010 Effects of plug-in hybrid electric vehicles on ozone concentrations in Colorado *Environ. Sci. Technol.* **44** 6256–62
[23] Pan S, Roy A, Choi Y, Eslami E, Thomas S, Jiang X and Gao H O 2019 Potential impacts of electric vehicles on air quality and health endpoints in the Greater Houston area in 2040 *Atmos. Environ.* **207** 38–51
[24] Razeghi G, Carreras-Sospedra M, Brown T, Brouwer J, Dabdub D and Samuelsen S 2016 Episodic air quality impacts of plug-in electric vehicles *Atmos. Environ.* **137** 90–100
[25] Skipper T N, Lawal A S, Hu Y and Russell A G 2023 Air quality impacts of electric vehicle adoption in California *Atmos. Environ.* **294** 119492
[26] Camilleri S, Montgomery A, Visa M, Schnell J, Adelman Z, Janssen M, Grubert E, Anenberg S and Horton D 2023 Air quality, health and equity implications of electrifying heavy-duty vehicles *Nat. Sustain.* 1–11
[27] Mohegh A, Goldberg D, Achakulwisut P and Anenberg S C 2020 Sensitivity of estimated NO_2-Attributable pediatric asthma incidence to grid resolution and urbanicity *Environ. Res. Lett.* **16** 014019
[28] LADCO 2022 Attainment demonstration modeling for the 2015 ozone national ambient air quality standard: technical support document (Lake Michigan Air Directors Consortium) p 132 (available at: www.ladco.org/wp-content/uploads/Projects/Ozone/ModerateTSD/LADCO_2015O3_ModerateNAASIP_TSD_21Sep2022.pdf)
[29] INRIX *Scorecard City* (Inrix) (available at: https://inrix.com/scorecard-city/)
[30] American Lung Association Most polluted cities | state of the Air (American Lung Association) (available at: www.lung.org/research/sota/city-rankings/most-polluted-cities)
[31] Byun D and Schere K L 2006 Review of the governing equations, computational algorithms, and other components of the Models-3 community multiscale air quality (CMAQ) modeling system *Appl. Mech. Rev.* **59** 51–77
[32] Skamarock W, Klemp J, Dudhia J, Gill D, Barker D, Wang W, Huang X-Y and Duda M 2008 A description of the advanced research WRF version 3 (UCAR/NCAR) p 1002
[33] Wong D C, Pleim J, Mathur R, Binkowski F, Otte T, Gilliam R, Pouliot G, Xiu A, Young J O and Kang D 2012 WRF-CMAQ two-way coupled system with aerosol feedback: software development and preliminary results *Geosci. Model Dev.* **5** 299–312
[34] Montgomery A, Schnell J L, Adelman Z, Janssen M and Horton D E 2023 Simulation of neighborhood-scale air quality with two-way coupled WRF-CMAQ over southern lake Michigan-Chicago region *J. Geophys. Res. Atmos.* **128** e2022JD037942
[35] LADCO Lake Michigan air director's consortium emissions (available at: www.ladco.org/technical/emissions/)
[36] Eyth A, Vukovich J, Farkas C and Madeleine S 2016 *Version 7.2 Technical Support Document* (US EPA) (available at: www.epa.gov/air-emissions-modeling/2016-version-72-technical-support-document) (https://doi.org/10.1021/acs.est.6b04752)
[37] Baek B and Seppanen C Sparse matrix operator kernel emissions (SMOKE) modeling system (Zenodo)
[38] EPA Motor Vehicle Emission Simulator (MOVES): User Guide for MOVES2014 (EPA-420-B-14-055) (available at: https://nepis.epa.gov/Exe/ZyPDF.cgi/P100JWAL.PDF?Dockey=P100JWAL.PDF)
[39] Liang X, Zhang S, Wu Y, Xing J, He X, Zhang K M, Wang S and Hao J 2019 Air quality and health benefits from fleet electrification in China *Nat. Sustain.* **2** 962–71
[40] Bloomberg EVO report 2022 BloombergNEF Bloomberg finance LP (BloombergNEF) (available at: https://about.bnef.com/electric-vehicle-outlook/)
[41] ICCT Racing to zero: the ambition we need for zero-emission heavy-duty vehicles in the United States (International Council on Clean Transportation) (available at: https://theicct.org/racing-to-zero-hdv-us-apr22/)
[42] Najman L *EV Adoption, Trends & Statistics in the US* (Recurrent) (available at: www.recurrentauto.com/research/ev-adoption-us)

[43] Grubert E and Hastings-Simon S 2022 Designing the mid-transition: a review of medium-term challenges for coordinated decarbonization in the United States *WIREs Clim. Change* **13** e768
[44] U.S. EPA 2021 EGRID technical guide with year 2019 data (U.S. Environmental Protection Agency) p 126 (available at: www.epa.gov/sites/default/files/2021-02/documents/egrid2019_technical_guide.pdf)
[45] Grubert E 2020 Fossil electricity retirement deadlines for a just transition *Science* **370** 1171–3
[46] Verma S, Dwivedi G and Verma P 2022 Life cycle assessment of electric vehicles in comparison to combustion engine vehicles: a review *Mater. Today Proc.* **49** 217–22
[47] Turner M C *et al* 2016 Long-term ozone exposure and mortality in a large prospective study *Am. J. Respir. Crit. Care Med.* **193** 1134–42
[48] Manson S, Schroeder J, Van Riper D, Kugler T and Ruggles S 2022 National historical geographic information system: version vol 17
[49] Industrial Economic, Incorporated 2022 Analysis of PM2.5-Related health burdens under current and alternative NAAQS (IEc) p 113 (available at: https://globalcleanair.org/files/2022/05/Analysis-of-PM2.5-Related-Health-Burdens-Under-Current-and-Alternative-NAAQS.pdf)
[50] WHO 2021 WHO global air quality guidelines: particulate matter (PM2.5 and PM10), ozone, nitrogen dioxide, sulfur dioxide and carbon monoxide (World Health Organization)
[51] Gugamsetty B, Wei H, Liu C-N, Awasthi A, Hsu S-C, Tsai C-J, Roam G-D, Wu Y-C and Chen C-F 2012 Source characterization and apportionment of PM10, PM2.5 and PM0.1 by using positive matrix factorization *Aerosol Air Qual. Res.* **12** 476–91
[52] Yang H, Huang X, Westervelt D M, Horowitz L and Peng W 2023 Socio-demographic factors shaping the future global health burden from air pollution *Nat. Sustain.* **6** 58–68
[53] Hess J J *et al* 2020 Guidelines for modeling and reporting health effects of climate change mitigation actions *Environ. Health Perspect.* **128** 115001
[54] Anenberg S C, Miller J, Henze D K, Minjares R and Achakulwisut P 2019 The global burden of transportation tailpipe emissions on air pollution-related mortality in 2010 and 2015 *Environ. Res. Lett.* **14** 094012
[55] Viscusi W K and Masterman C J 2017 Income elasticities and global values of a statistical life *J. Benefit-Cost Anal.* **8** 226–50
[56] Rennert K *et al* 2022 Comprehensive evidence implies a higher social cost of CO_2 *Nature* **610** 687–92
[57] Tol R S J 2023 Social cost of carbon estimates have increased over time *Nat. Clim. Change* **13** 532–6
[58] IWG, U.S. Government 2021 Technical support document: social cost of carbon, methane, and nitrous oxide interim estimates under executive order 13990 (available at: www.whitehouse.gov/wp-content/uploads/2021/02/TechnicalSupportDocument_SocialCostofCarbonMethaneNitrousOxide.pdf)
[59] Shindell D *et al* 2021 Temporal and spatial distribution of health, labor, and crop benefits of climate change mitigation in the United States *Proc. Natl Acad. Sci. USA* **118** e2104061118
[60] Qian Y *et al* 2021 Long-term exposure to low-level NO_2 and mortality among the elderly population in the southeastern United States *Environ. Health Perspect.* **129** 127009
[61] Wolf K *et al* 2021 Long-term exposure to low-level ambient air pollution and incidence of stroke and coronary heart disease: a pooled analysis of six European cohorts within the ELAPSE project *Lancet Planet. Health* **5** e620–32
[62] Stieb D M, Berjawi R, Emode M, Zheng C, Salama D, Hocking R, Lyrette N, Matz C, Lavigne E and Shin H H 2021 Systematic review and meta-analysis of cohort studies of long term outdoor nitrogen dioxide exposure and mortality *PLoS One* **16** e0246451
[63] Emery C, Liu Z, Russell A G, Odman M T, Yarwood G and Kumar N 2017 Recommendations on statistics and benchmarks to assess photochemical model performance *J. Air Waste Manage. Assoc.* **67** 582–98
[64] Chang S Y, Huang J, Chaveste M R, Lurmann F W, Eisinger D S, Mukherjee A D, Erdakos G B, Alexander M and Knipping E 2023 Electric vehicle fleet penetration helps address inequalities in air quality and improves environmental justice *Commun. Earth Environ.* **4** 1–15
[65] Zhang X, Just A C, Hsu H H L, Kloog I, Woody M, Mi Z, Rush J, Georgopoulos P, Wright R O and Stroustrup A 2021 A hybrid approach to predict daily NO_2 concentrations at city block scale *Sci. Total Environ.* **761** 143279
[66] Lv Z, Luo Z, Deng F, Wang X, Zhao J, Xu L, He T, Zhang Y, Liu H and He K Development and application of a multi-scale modeling framework for urban high-resolution NO_2 pollution mapping (available at: https://acp.copernicus.org/articles/22/15685/2022/acp-22-15685-2022-discussion.html) (Accessed 14 June 2023)
[67] Giles-Corti B *et al* 2016 City planning and population health: a global challenge *Lancet* **388** 2912–24
[68] Nieuwenhuijsen M J 2020 Urban and transport planning pathways to carbon neutral, liveable and healthy cities; a review of the current evidence *Environ. Int.* **140** 105661